Flight Dynamics and Control of Rocket Assisted Quadrotor

Salahudden Salahudden[1*], *Prabhjeet Singh*[1], *Rakesh Kumar*[2], *Yogendra Chhetri*[3] and *Tushar Siag*[4]

[1]Assistant Professors, Aerospace Engineering Department, Punjab Engineering College, Chandigarh, Punjab 160012, India
[2]Professor, Aerospace Engineering Department, Punjab Engineering College, Chandigarh, Punjab 160012, India
[3]Joint Director, Space Operations, Ministry of Defence, Delhi, 110010, India
[4]Graduate Research Assistant, Mechanical and Aerospace Engineering Department, Florida State University, Tallahassee, 32306, USA

Abstract. After a high-speed flight, the immediate hovering is always challenging due to system inertia. This requires an accurate dynamic model and robust control design. In this paper, the flight dynamic model of a rocket-assisted quadrotor is developed. The flight control using the classical approach is designed to perform the required mission. The task is to launch from one particular location, fly as a rocket for a fixed time, and then follow the hovering command. The transition from rocket like vertical climb to quadrotor flight mode is facilitated by the coordinated action of the rotors of a quadcopter. Achieving the smooth shift between these flight regimes depends on many key parameters such as velocity, rotor thrust, and overall system power. The transition is generally influenced by parameters such as a distance covered and duration of a flight. Simulation results indicated that with the proposed flight controller, vehicle is able to decelerate appropriately and maintain stable hovering at the designated altitude. The flight simulation framework also demonstrated potential for guiding the development and evaluation of a small-scale prototype.

1 Introduction

In recent years, there has been significant surge in attention toward the rotary-wing Unmanned Aerial Vehicles (UAVs) among researchers, engineers, as well as professionals from both industry and an academia [1]. Among these, the quadrotor which commonly known as a quadcopter has gained particular attention due to several advantages over other the types of UAV . These include its compact design, relatively simple due to its mechanical structure, vertical take-off and landing (VTOL) capability, and enhanced agility and maneuverability [2]. Owing to these characteristics, quadrotors are increasingly being deployed in the wide range of applications such as mapping and rescue missions, infrastructure inspections, aerial payload delivery, defense operations, and atmospheric

* Corresponding author: qazisalahudden@gmail.com

research [3]. Achieving full autonomy in the quadrotor demands exceptionally accurate and agile control mechanism. However, designing such controller presents significant challenges as the quadrotor exhibits strong nonlinear and uncertain dynamics and underactuated behavior, making control design a complex and active area of research [4,5].

Conversely, the small short-range rocket serves as compact and efficient aerospace platform, specifically engineered for missions that demand limited altitude and range capabilities. These rockets are typically used for applications such as atmospheric research, technology testing, educational experiments, and military purposes [6]. Short-range rockets, utilizing either solid or liquid propellants, offer the low-cost and easily deployable solution for quick access to a targeted altitudes or regions [7]. Their small size and limited range make them ideal for localized studies, such as measuring atmospheric conditions, testing sensors, or conducting short-duration experiments. Additionally, their streamlined design and operational simplicity allow for quick preparation and launch, making them a versatile and accessible solution for both scientific and commercial applications [8,9].

First, focusing on the control of quadrotors, various attempts have been made to apply robust control techniques for quadrotor control. Amongst them, sliding mode control (SMC) is a very popular control tool that can handle nonlinear systems [10,11]. If designed properly, SMC shows insensitivity to model errors, parametric uncertainties, and other external disturbances [12–14]. Xu et al. [15] proposed an SMC design philosophy that could be applied to a class of under-actuated systems that are in the cascaded form, including quadrotors. Further, Ning et al. [16,17] designed SMC and adaptive integral-based sub-controllers by addressing under-actuation and cascade constraints for a quadrotor system. Based on the SMC design approach given [18], Zheng et al. [19] designed a second-order SMC (2-SMC) for the position and attitude tracking of a quadrotor. Not only nominal conditions, but SMC also showed superior performance in addressing the aircraft loss of control problem [20-24].

Effective control systems are crucial to maintaining a stability and maneuverability of the quadrotor, particularly in the presence of dynamic disturbances and an inherently nonlinear nature of its flight behavior. Among the numerous control strategies, the Proportional-Integral-Derivative (PID) controller remains the most widely used due to its simplicity, ease of implementation, and robust performance in real-time applications [25]. The PID controller functions within the feedback loop, reducing the difference between a desired setpoint and the actual system output through the combined use of proportional, integral, and derivative actions. The proportional component (P) of a PID controller addresses present errors, the integral term (I) helps eliminate steady-state discrepancies by accounting for accumulated past errors, and the derivative term (D) anticipates future error trends, thereby improving the system's responsiveness [26]. In quadrotor applications, PID controllers are commonly employed across multiple control loops—such as those managing roll, pitch, yaw, and altitude, to maintain consistent stability and precision throughout flight.

While PID controllers are widely favored for their easy implementation and reliable real-time response, they often struggle with systems that are highly nonlinear and uncertain. To overcome these challenges, various researchers have introduced tuning approaches, ranging from traditional techniques such as Ziegler-Nichols to more recent heuristic based methods [27]. In addition, hybrid schemes that combine PID control with fuzzy logic or neural networks have shown promise in mitigating impact of disturbances and improving adaptability [28]. Nonetheless, PID control remains cornerstone in UAV systems due to its balance between simplicity and effectiveness.

This paper introduces the novel hybrid concept that integrates structural characteristics of rocket with maneuverability of quadrotor. The proposed system employs rocket body augmented with a quadrotor mechanism; featuring four rotors symmetrically mounted around central part. This integration is designed to capitalize on vertical takeoff and landing

capabilities of multirotor UAVs, while retaining a speed and range benefits of a propulsion of rocket. The quadrotor module improves control accuracy during critical stages like takeoff, mid-flight maneuvering, and landing tasks that are typically more challenging to handle in the standard rocket systems. This approach proves especially useful in missions requiring accurate landings, reusable flight paths, or targeted payload delivery to remote or constrained environments.

By merging the agility of quadcopters with the power of rockets, the system opens up new avenues in aerospace applications ranging from space exploration to tactical aerial missions. The control of this hybrid platform is achieved using a PID based approach, which has been shown in prior studies to offer reliable performance across various operating conditions. In this study, PID controllers are used to simulate and validate control strategy under different flight scenarios.

The key innovation of this work lies in its integrated simulation of flight dynamics and control for the hybrid system. The combined behavior of the rocket and quadrotor is modeled within a single dynamic framework, allowing for comprehensive control strategy development. Simulation results confirm that the system performs well during launch and maneuvering phases, demonstrating both feasibility and effectiveness. This unique design effectively bridges a gap between multirotor drones and high-speed, high-altitude vehicles. Rocket propulsion enables a vehicle to perform swift vertical climbs and operate within broader flight envelopes capabilities that exceed those of conventional drones. This study also explores an intricate control difficulty introduced by this hybrid configuration and presents stabilization techniques specifically designed to manage these challenges. Overall, this research not only expands theoretical understanding but also showcases a viable path toward real-world implementation. The proposed system highlights significant potential for both civilian and defense applications, representing a meaningful step forward in an aerial robotics and hybrid flight technologies.

The proposed work is structured as follows: The flight model is presented in the next section. Thereafter, dynamic equations are discussed. Subsequent section illustrates the flight control law. Obtained results are discussed is then discussed. Last section houses concluding remarks.

2 Proposed Model

Figure 1 illustrates a vertical takeoff system featuring a central cylindrical body with the four arms extending outward in cross configuration. Each arm ends with the propeller, forming a layout similar to quadcopter. The design reflects the fusion of conventional drone and rocket elements, indicating the intent to achieve both stable vertical ascent and sustained hovering capability. The main body is expected to contain important hardware, including the power supply, electronic control units, and other key systems. The physical characteristics of the model is shown in Table 1.

Fig. 1. Schematic of the proposed model.

Table 1. Physical characteristics of model.

Design Parameters	Values
Model mass, m	$10\ kg$
Rocket fuel mass, m_f	$3\ kg$
Roll inertia, I_{xx}	$2.1\ kg\ m^2$
Pitch inertia, I_{yy}	$2.7\ kg\ m^2$
Yaw inertia, I_{zz}	$4.5\ kg\ m^2$
Model length, l	$1.0\ m$
Quadrotor arm length, l_{quad}	0.6
Thrust constant, K_{T_i} $(i = 1,2,3,4)$	1.533×10^{-4}
Torque constant, K_d	1.386×10^{-5}

3 Flight Dynamic Model

In this section, a **flight dynamic model** is presented to describe the motion of the proposed model. For rockets, the model accounts for forces such as thrust, drag, gravity, and changing mass due to fuel consumption, while for quadrotors, it incorporates aerodynamic forces, thrust generated by rotors, and moments that control pitch, roll, and yaw. These models use equations of motion to simulate the dynamics and behavior of the proposed model. In this paper, the flight dynamic models will be used to analyze stability, control, and performance.

3.1 Rocket Model

The equation representing the translation (Eq. (1)) and rotational (Eq. (2)) motion of the aircraft can be written as [29]

$$\dot{V} = \frac{1}{m}(F_{total} - \omega \times m\,V) \tag{1}$$

$$\dot{\omega} = I^{-1}(M_{total} - \omega \times I\omega) \tag{2}$$

where m, V, ω are the aircraft mass, total velocity, and angular velocity of an aircraft. In Eq. (1) and (2), the total force and total moment, respectively, can be expanded as

$$F_{total} = F_{aero} + F_{prop} + F_{grav} \tag{3}$$

$$M_{total} = M_{aero} + M_{prop} \tag{4}$$

where F_{aero} and M_{aero} are the aerodynamic forces and moments, respectively, can be written as

$$F_{aero} = \begin{bmatrix} X_{aero} \\ Y_{aero} \\ Z_{aero} \end{bmatrix} = \begin{bmatrix} C_X \\ C_Y \\ C_Z \end{bmatrix} \bar{q}S \tag{5}$$

$$M_{aero} = \begin{bmatrix} L_{aero} \\ M_{aero} \\ N_{aero} \end{bmatrix} = \begin{bmatrix} bC_l \\ \bar{c}C_m \\ bC_n \end{bmatrix} \bar{q}S \tag{6}$$

where C_l, C_m and C_n are roll, pitch, and yaw moment coefficients. The C_X, C_Y and C_Z are the force coefficients in the body axis. These are obtained from the wind frame reference frame by Eq. (7) [30, 31].

$$\begin{bmatrix} C_X \\ C_Y \\ C_Z \end{bmatrix} = R_1 R_2 \begin{bmatrix} -C_D \\ -C_Y \\ -C_L \end{bmatrix} \tag{7}$$

where C_L and C_D are the lift and drag coefficients, respectively. The R_1 and R_2 are the rotation matrix with angle of attack (α) and side slip angle (β), respectively.

$$R_1 = \begin{bmatrix} \cos\alpha & 0 & -\sin\alpha \\ 0 & 1 & 0 \\ \sin\alpha & 0 & \cos\alpha \end{bmatrix}, R_2 = \begin{bmatrix} \cos\beta & -\sin\beta & 0 \\ \sin\beta & \cos\beta & 0 \\ 0 & 0 & 1 \end{bmatrix}$$

3.2 Quad Rotor Model

Let $, I_1 = (I_{yy} - I_{zz})/I_{xx}, I_2 = (I_{zz} - I_{xx})/I_{yy}, I_3 = (I_{xx} - I_{yy})/I_{zz},$ where I_{xx}, I_{yy} and I_{zz}, respectively, represent the roll, pitch and yaw moment of inertia of the quadrotor and I_r is the rotor inertia. The control inputs are defined as $[u_1\ u_2\ u_3\ u_4]^T = [F\ \tau_\phi\ \tau_\theta\ \tau_\psi]^T \in \mathbb{R}^4$. The quadrotor dynamics is then given by (1) under the following assumptions: 1) The centre of gravity of the quadrotor coincides with the origin of the body axis of the quadrotor frame, 2) The quadrotor has axis symmetry, and 3) Since quadrotor design speed is low, the aerodynamics drag of quadrotor is not included in the control feedback loop. However, the drag effect is included in the dynamic equations of a quadrotor.

$$\left.\begin{aligned} \ddot{x} &= \left(C_\phi S_\theta C_\psi + S_\phi S_\psi\right)\frac{u_1}{m} - K_x\frac{\dot{x}}{m} \\ \ddot{y} &= \left(C_\phi S_\theta S_\psi - S_\phi C_\psi\right)\frac{u_1}{m} - K_y\frac{\dot{y}}{m} \\ \ddot{z} &= g - \left(C_\phi C_\theta\right)\frac{u_1}{m} + K_z\frac{\dot{z}}{m} \\ \ddot{\phi} &= qrI_1 - \frac{I_r}{I_{xx}}q(\omega_1 - \omega_2 + \omega_3 - \omega_4) + \frac{1}{I_{xx}}u_2 \\ \ddot{\theta} &= prI_2 + \frac{I_r}{I_{xx}}p(\omega_1 - \omega_2 + \omega_3 - \omega_4) + \frac{1}{I_{yy}}u_3 \\ \ddot{\psi} &= pqI_3 + \frac{1}{I_{zz}}u_4 \end{aligned}\right\} \tag{8}$$

where $S_{(.)}$, $C_{(.)}$, $T_{(.)}$ = $\sin(.)$, $\cos(.)$ and $\tan(.)$, respectively and $K_i, i = x, y, z$ are the coefficients to model the drag term.

4 Flight Control Law Design

This section presents the control design for quadrotor control. The traditional PID controller is used to design all control loops. These loops typically include inner and outer control loops. The inner loop, or attitude control loop, stabilizes the quadrotor by controlling its roll, pitch, and yaw angles using fast-response sensors like gyroscopes. The position control loop, often referred to as an outer loop, manages high-level objectives like maintaining altitude and controlling horizontal movement by supplying reference inputs to an inner loop. In most quadrotor systems, each control loop commonly employs a PID controller to reduce error and ensure accurate system responses. This hierarchical control structure contributes to smooth and stable flight, even when operating in rapidly changing or unpredictable conditions. The proportional (P) component addresses the current error, the

integral part (I) accounts for past errors to eliminate long-term drift, and the derivative term (D) anticipates future trends by responding to rate of change. In particular, the derivative action support to dampen sudden variations, reducing the risk of overshooting a target.

4.1 Altitude Control Design

Controlling altitude of quadrotor depends on a PID controller to regulate vertical movement by finetuning the thrust generated by all rotors. This is achieved by continuously comparing desired altitude (height) with real-time altitude data taken from onboard sensors (for example, barometers). The resulting error is processed using proportional, integral, and derivative components, which together determine corrective thrust needed to control the motion. This approach helps maintain accurate and stable altitude control, even when faced with external disturbances. The control strategy can be written mathematically as

$$u_h = k_p(h_d - h) + k_{i_p}\int_0^t (h_d - h)d\tau + +k_{d_h}\left(\dot{h}_c - \dot{h}\right) \tag{9}$$

4.2 Lateral Control Design

To maintain stability and control over the quadrotor's roll motion, PID controller is commonly employed to manage angular displacement around longitudinal axis. This control strategy involves continuously monitoring a difference between desired roll angle and actual one, using data from onboard sensor like gyroscopes and accelerometers. To correct roll and maintain stable flight, a controller adjusts a thrust of diagonally opposite rotor pairs in the response to detected imbalances. The process of the control law can be represented mathematically as:

$$u_\phi = k_p(p_d - p) + k_{i_p}\int_0^t (p_d - p)d\tau \tag{10}$$

The commanded roll rate is obtained as

$$p_d = k_\phi(\phi_d - \phi) + k_{i_\phi}\int_0^t (\phi_d - \phi)d\tau \tag{11}$$

The commanded roll angle is obtained as

$$\phi_d = k_{V_Y}\left(V_{Y_d} - V_Y\right) + k_{i_{V_Y}}\int_0^t \left(V_{Y_d} - V_Y\right)d\tau \tag{12}$$

The commanded lateral velocity is obtained as

$$V_{Y_d} = k_Y(Y_d - Y) + k_{i_Y}\int_0^t (Y_d - Y)d\tau \tag{13}$$

4.3 Directional Control Design

Heading control in a quadrotor, achieved through a PID controller, is responsible for regulating the yaw angle ensuring the vehicle maintains a correct orientation around its vertical axis. The controller determines a deviation between a target heading and a current yaw angle, which is usually obtained from onboard instruments like gyroscopes or magnetometers. Based on this error, the PID algorithm adjusts the torque by varying the speeds of opposing rotor pairs, enabling smooth and precise yaw corrections. This allows quadrotor to either hold the steady heading or execute controlled directional changes. Mathematically, yaw control can be described as

$$u_\psi = k_p(r_d - r) + k_{i_p}\int_0^t (r_d - r)d\tau \tag{14}$$

The commanded yaw rate is determined as

$$r_d = k_\psi(\psi_d - \psi) + k_{i_\theta}\int_0^t (\psi_d - \psi)d\tau \tag{15}$$

where k represents the controller gain.

4.4 Control Architecture

Figure 2 shows complete control system of quadrotor. As illustrated, quadrotor control relies on the series of nested feedback loop to maintain stability, achieve accurate motion, and allow for agile maneuvering during flight. These loops include rate control, attitude control, velocity control, position control, and altitude control. In the core, rate control loop is the innermost which adjusts the rotational speed of the individual motors to control roll, pitch, and yaw rates. This loop operates under the command of the attitude control loop. Data from onboard sensors such as accelerometers and gyroscopes feed into both control loops, enabling a system to monitor angular velocity and orientation and perform real-time corrective actions. The velocity loop, in turn, feeds into altitude control loop, which maintains vertical position. In outer loop, the position control loop governs horizontal movement, fine-tuning motor speeds to navigate and maintain the quadrotor's location in space.

The required velocity is computed based on the desired and actual position, which is then compared to the actual one, and the desired attitude (roll and pitch) is determined. The altitude control loop regulates the vertical position of the quadrotor by adjusting the collective thrust of the rotors, ensuring that the drone maintains a consistent altitude or climbs/descent as required.

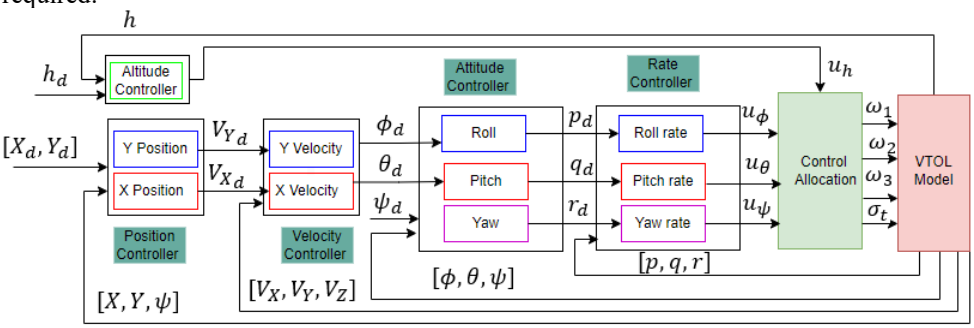

Fig. 2. Control architecture.

5 Results and Discussions

The model is launched from mean sea level (altitude, $h = 0$ m) as shown in Figure 1. The rocket flight is up to 7 seconds; after that, that quad mode is activated. Figure 1a illustrates the altitude profile of a system over time, highlighting two distinct flight phases: Rocket-Assisted Launch and the Quadrotor Flight. The x-axis represents time in seconds (s), while the y-axis shows altitude h in meters (m). The system begins with a steep climb during the rocket-assisted launch, reaching its peak altitude of around 70 meters in approximately 8-10 seconds. This phase is marked with a green label and a vertical red dotted line, signifying the transition point. After the launch phase, the altitude decreases before stabilizing into oscillations, which characterize the quadrotor flight phase (marked with a magenta label). During this phase, the system experiences a series of altitude adjustments, exhibiting peaks and valleys as it maintains controlled flight. By the end of the observed 50-second duration, the altitude stabilizes at around 50 meters (commanded height), demonstrating the system's transition from powered launch to sustained quadrotor operation. Figure 3b depicts the

airspeed (V) of a system. The graph shows a sharp increase in airspeed during the initial phase, where the velocity peaks at around 75 m/s before rapidly decreasing. Once the quad mode is activated, the flight controller pitches the quad up to reduce the speed to make it hover at the desired set points. Following this, the airspeed stabilizes to lower values, with oscillations indicating adjustments or disturbances before settling into a more stable flight profile. The subsequent phase demonstrates consistent airspeed over time, suggesting steady quadrotor operation. This graph highlights the performance transition from a high-thrust launch phase to a more controlled, steady flight phase.

Figure 3c depicts the pitch rate (q) (in degrees per second). The pitch rate starts at a high positive value before 10 seconds, likely corresponding to a "Rocket Assisted Launch" phase. At the 10-second mark, a sharp decline occurs, and the pitch rate becomes negative, reaching its lowest value of approximately -30 deg/s shortly after the transition, signifying a significant change in dynamics. After this, the pitch rate begins to recover, oscillating and eventually stabilizing into a smoother profile. In the post-launch segment, where the pitch rate oscillates with a peak and gradually reduces in magnitude. The graph covers a time range up to 50 seconds, showing the system's transition from a high-intensity launch phase to a stabilized quadrotor flight phase. Figure 3d shows the pitch angle (θ) (in degrees). During the initial phase, the pitch angle rapidly increases, peaking around 60 degrees just before 10 seconds. At the 10-second mark, there is a sudden transition, and the pitch angle sharply decreases, reaching a minimum of approximately -60 degrees shortly after. This indicates a drastic change in the flight dynamics following the rocket-assisted launch. In the second phase, the pitch angle begins to stabilize, oscillating with diminishing magnitude as the system recovers. By the end of the observed time (50 seconds), the pitch angle trends toward a relatively steady state. This graph clearly illustrates the system's transition from a high-pitch launch phase to a more controlled quadrotor flight phase.

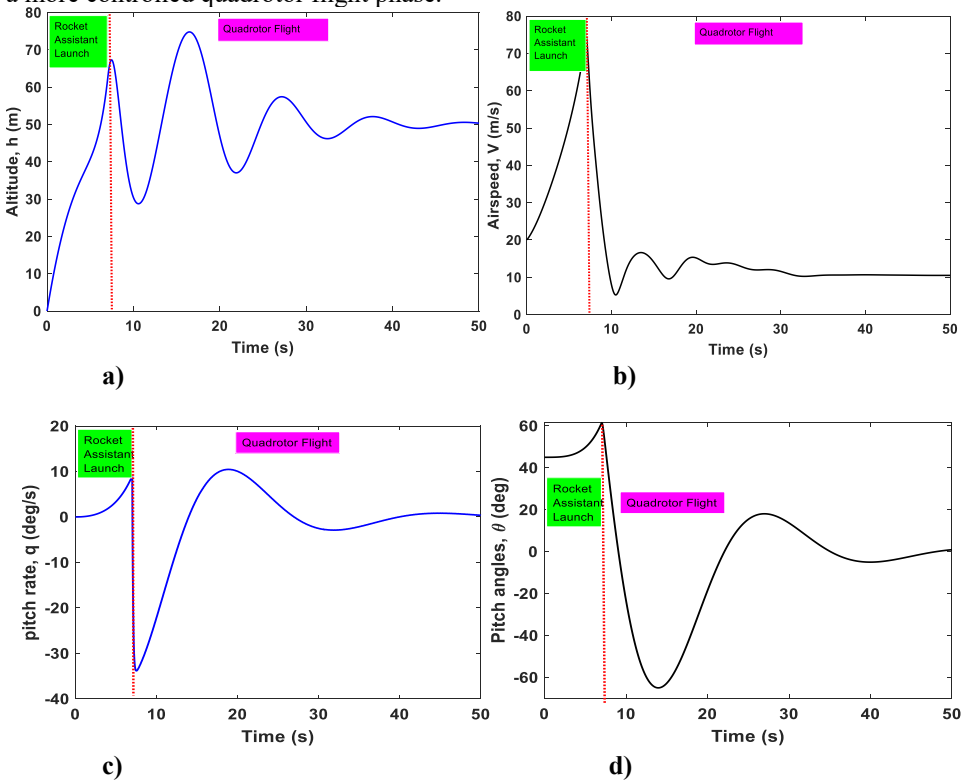

Fig. 3. Flight profile: a) altitude and b) flight velocity.

This set of four graphs displays the rotor RPM (N_1, N_2, N_3) and (N_4)as a function of time (in seconds) for system undergoing a "Rocket Assisted Launch" followed by "Quadrotor Flight." Each graph corresponds to one of the four rotors, with similar trends observed across all plots. During the initial "Rocket Assisted Launch" phase (highlighted in green), the rotor RPM remains high and relatively steady, maintaining around 6000 RPM before the 10-second mark. At the 10-second point, marked by a red dotted line, there is a sharp drop in rotor speed, indicating a transition to the "Quadrotor Flight" phase (highlighted in pink). In this phase, the rotor speeds exhibit oscillatory behavior as the system stabilizes. Over time, the rotor RPM shows a gradual settling trend, with oscillations reducing in magnitude. This behavior reflects the dynamic adjustment of the rotors to stabilize the quadrotor's flight after the abrupt transition from the rocket-assisted launch. The similar patterns across all four graphs indicate synchronized rotor behavior during both phases of the flight.

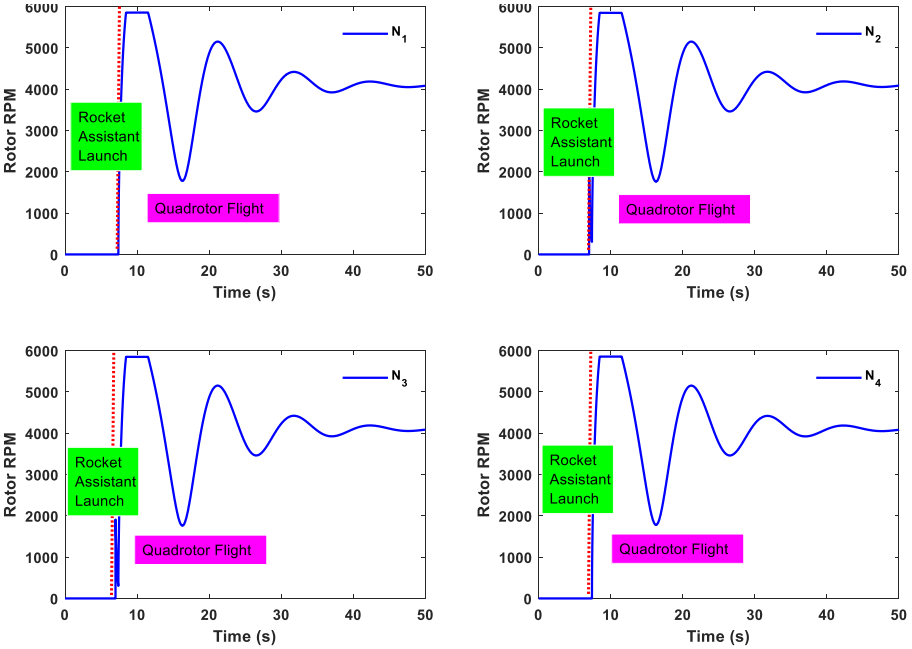

Fig. 4. Quadrotor RPM.

6 Conclusions

This study presents the flight dynamics model of a rocket-assisted quadrotor. A conventional technique of flight control was used to complete the needed mission. It was found that the model can hover at the specified set point and lower its speed while using the designed flight controller. The successful launch from a specific position, rocket flight, and finally, the hover was achieved. In flight, quadcopter rotors successfully transitioned from rocket to quadrotor flight smoothly. It was seen that transition logic based on the distance traveled and the time available is successfully implemented on the flight simulation level.

In the future, the proposed control approach could be tested on a smaller-scale model. The designed controller can also be used to provide the required recovery commands in an automated manner. Furthermore, sensor models with delays and aircraft model perturbations can be included to test the resilience of the proposed work. The scaling challenges are important for practical relevance. In future work, there are key issues such as Reynolds number effects, differences in aerodynamic scaling, actuator resolution and sensor noise.

These issues can be addressed by employing appropriate scaling laws, controller tuning for dynamic response mismatch and validating performance through careful experimental design.

References

1. A. Tayebi, S. McGilvray, Attitude stabilization of a VTOL quadrotor aircraft. *IEEE Trans. Control Syst. Technol.* 14, 562–571 (2006).
2. C. Nicol, C. J. B. Macnab, A. Ramirez-Serrano, Robust adaptive control of a quadrotor helicopter. *Mechatronics* 21, 927–938 (2011).
3. E.-H. Zheng, J.-J. Xiong, J.-L. Luo, Second order sliding mode control for a quadrotor UAV. *ISA Trans.* 53, 1350–1356 (2014).
4. X. Wang, S. Sun, E. J. van Kampen, Q. Chu, Quadrotor fault-tolerant incremental sliding mode control driven by sliding mode disturbance observers. *Aerosp. Sci. Technol.* 87, 417–430 (2019).
5. J.-J. Xiong, E.-H. Zheng, Position and attitude tracking control for a quadrotor UAV. *ISA Trans.* 53, 725–731 (2014).
6. G.P. Sutton, O. Biblarz, *Rocket Propulsion Elements*, 9th ed. (Wiley, 2016).
7. J. Parker, Applications of suborbital rockets for atmospheric studies. *J. Aerosp. Sci.* (2020).
8. G.D. Francesco, M. Mattei, Modeling and incremental nonlinear dynamic inversion control of a novel unmanned tiltrotor. *J. Aircr.* 53, 73–86 (2016).
9. C. Anderson, R. Torres, P. Green, AI-assisted sensor fusion for hybrid UAV navigation. *IEEE Trans. Aerosp. Electron. Syst.* 60(2), 2245–2260 (2024).
10. P. Singh, D.K. Giri, A.K. Ghosh, Robust sliding mode augmenting integral backstepping for lateral-directional control of a highly maneuverable aircraft. *Proc. Inst. Mech. Eng. G J. Aerosp. Eng.* 237, 2428–2441 (2023).
11. P. Singh, S. Salahudden, D.K. Giri, A.K. Ghosh, Attitude control of Hansa-3 aircraft with perturbation using sliding-mode controller. In: *IEEE Aerospace Conference Proceedings* (2022).
12. V.I. Utkin, *Sliding Modes in Control and Optimization* (Springer Science & Business Media, 2013).
13. Q. Zhu, Complete model-free sliding mode control (CMFSMC). *Sci. Rep.* 11, (2021).
14. N. Ebrahimi, S. Ozgoli, A. Ramezani, Model-free sliding mode control: theory and application. *Proc. Inst. Mech. Eng. I J. Syst. Control Eng.* 232, 1292–1301 (2018).
15. R. Xu, Ü. Özgüner, Sliding mode control of a class of underactuated systems. *Automatica* 44, 233–241 (2008).
16. N. Wang, S.F. Su, M. Han, W.H. Chen, Backpropagating constraints-based trajectory tracking control of a quadrotor with constrained actuator dynamics and complex unknowns. *IEEE Trans. Syst. Man Cybern. Syst.* 49, 1322–1337 (2019).
17. N. Wang, Q. Deng, G. Xie, X. Pan, Hybrid finite-time trajectory tracking control of a quadrotor. *ISA Trans.* 90, 278–286 (2019).
18. J.E. Slotine, L. Weiping, *Applied Nonlinear Control* (Prentice-Hall, New Jersey, 1991) pp. 207–246.
19. E.-H. Zheng, J.-J. Xiong, J.-L. Luo, Second order sliding mode control for a quadrotor UAV. *ISA Trans.* 53, 1350–1356 (2014).
20. S. Salahudden, V.S. Dwivedi, P.N. Dwivedi, D.K. Giri, A.K. Ghosh, Aircraft flat-spin recovery using sliding-mode based attitude and altitude control. *Proc. Inst. Mech. Eng. G J. Aerosp. Eng.* 235, 924–936 (2021).
21. S. Salahudden, A.K. Ghosh, Robust control design based aircraft flat-spin recovery

using optimally deflected novel deployable fin. *Aerosp. Sci. Technol.* 115, 106823 (2021).
22. S. Salahudden, A.T. Das, A.K. Ghosh, Sliding-mode control and strategic thrust-vectoring based aircraft flat spin recovery with altitude loss minimization. *IEEE Trans. Aerosp. Electron. Syst.* 58, 3271–3282 (2022).
23. S. Salahudden, A.K. Ghosh, Vertical thrust-based effective flat-spin recovery of aircraft restricting altitude loss. *Proc. Inst. Mech. Eng. G J. Aerosp. Eng.* 236, 3567–3575 (2022).
24. S. Salahudden, Impact of wind and wind shear on sliding mode controller assisted aircraft spin recovery. *Control Eng. Pract.* 145, 105872 (2024).
25. K.J. Åström, T. Hägglund, *Advanced PID Control* (ISA – The Instrumentation, Systems, and Automation Society, 2006).
26. N.S. Nise, *Control Systems Engineering* (John Wiley & Sons, 2020).
27. Z. Shao, Y. Li, H. Zhang, Tuning PID controllers for UAV systems: a heuristic approach. *J. Control Theory Appl.* 16, 243–252 (2018).
28. H. Pathak, V. Kumar, V. Gupta, Hybrid PID–fuzzy logic control for stabilization of quadrotors. *Int. J. Intell. Syst. Appl.* 9, 23–30 (2017).
29. W.B. Randal, W.M. Timothy, *Navigation, Guidance and Control of Small Unmanned Aircraft* (Princeton University Press, New Jersey, 2012) pp. 1–72.
30. F.O. Smetana, D.C. Summey, W.D. Johnson, Riding and handling qualities of light aircraft – a review and analysis. *NASA CR-1975* (March 1972).
31. B.N. Pamadi, *Performance, Stability, Dynamics, and Control of Airplane*, 2nd ed. (AIAA Education Series, Virginia, 2004) pp. 631–694.